Research Article – Vol. 01, Issue 02, No. 07

Advanced in Engineering and Intelligence Systems

Journal Web Page: https://aeis.bilijipub.com

# Novel hybrid radial based neural network model on predicting the compressive strength of long-term HPC concrete

Hanlie Cheng[1,2,*] ,Shiela Kitchen[3] ,Graciela Daniels[4]

[1] *Faculty of Contemporary Sciences and Technologies, South East European University, Ilindenska 335, 1200 Tetovo, Macedonia*
[2] *COSL-EXPRO Testing Services (Tianjin) Co., Ltd., Tianjin 300457, China*
[3] *College of Arts and Sciences, University of New England, Armidale, NSW 2351, Australia*
[4] *Central Arizona College, Coolidge 85128, AZ, United States*

## Highlights

- The effect of fly ash and micro-silica on the compressive strength of HPC concrete was investigated.
- Two hybrid models based on RBFN and tuned by ALO and AOA optimization algorithms were developed.
- The prediction of compressive strength through artificial intelligence method delivers a valuable model.
- The training phase of the AORBFN model performed best in predicting compressive strength.
- The best $R^2$ value for the AORBF and the ALRBF model are 0.9706, and 0.9669 in the test phase.

**Article Info**

Received: 05 May 2022
Received in revised: 03 July 2022
Accepted: 06 July 2022
Available online: 07 July 2022

**Keywords**

Compressive strength,
HPC concrete,
arithmetic optimization,
antlion optimization,
radial base neural networks

**Abstract**

The additives' usage like micro-silica (MS) and fly ash (FA) through partial substitution of cohesive materials in concrete design has positive impacts on the concrete's mechanical properties, reducing concrete production cost and declining environmental pollution. The concrete's compressive strength is the main factor considered in the mechanical properties of the concrete, which is estimated by experimental efforts or non-destructive models as developed artificial models. In the present work, two hybrid radial base neural networks (RBFN) coupled with arithmetic optimization algorithm (AORBFN) and antlion optimization algorithm (ALRBFN) were developed for the prediction of compressive strength. The models' variables contain the binder, fly ash, micro-silica, superplasticizer, coarse aggregate, water, and the target's curing time as input and compressive strength. The results showed that both models have the capability of delivering a precise compressive strength prediction. The best $R^2$ value for the AORBF is 0.9706 in the test phase, and the best obtained $R^2$ for the ALRBF model is 0.9669, which is achieved in the same phase. The results conclude that the AORBF model can be preferred as an applicable model for compressive strength prediction.

## 1. Introduction

Concrete is the foundation for structures and has a large appliance in construction industries. Different mix designs choosing appropriate materials are introduced for concrete, considering functionality, toughness, eco-saving, weight, and workability. Construction properties of materials, especially the unusual cohesive material, depend on various factors like homogeneity of their segments, naturally different properties of diverse components, or possible contradictory effects of defined materials on the performance of the concrete [1–3] Several cohesive admixtures such as micro-silica, fly ah, nano-silica, and metakaolin is the most applied artificial admixtures for different purposes [4,5].

Fly ash is identical to usual Portland cement in size and shape and diminishes the percentage of water in the concrete mixtures. The appropriate mix of fly ash and superplasticizers in the concrete mixtures leads to enhancement in concrete properties, namely durability, strength properties, workability, permeability, and financial cost. The common way of applying fly ash is combining a proper percent of flu ash with the binder

* Corresponding Author: Hanlie Cheng
Email: chenghanlie@mau.edu.mk

material of the concrete to reach an environmentally friendly, eco-saving mix design. The decline of air pollution through decreasing the co2 emission of concrete admixed with fly ash is the environmental aspect. Also, concretes admixed with fly ash results a raise in compressive strength of concrete [6–8]. The common range of fly ash substitution percentage with the cohesive material of the concrete is 20% to 50%. Also, if the first day strength of concrete is negligible, the percentage of fly ash replacement can improve as much as 60% [9,10].

The size of the silica makes it possible to use it not only as filler but also as pozzolan in the concrete mixture [11]. Despite the enhancement of the short-term properties of concrete, such as compressive strength, rising the percentage of micro-silica percentage causes a reduction in the workability of the admixed concrete [12]. The pozzolanic feature feedback and the micro-silica particle size improve the concrete properties [13–18]. A common way to obtain less porosity in the concrete mixture is to use micro-silica with an appropriate percentage of superplasticizer where it helps increase the compressive strength of the concrete [19–21]. In an investigation, the effect of admixing micro-silica on self-consolidating concrete in the sulfuric acid medium was studied which the cohesive cement was replaced by micro-silica about 9%. The study results declared that adding micro-silica has a considerable effect on the compressive strength of concrete [22,23].

Experimental construction of different samples of concrete with various admixtures to estimate their effects on the compressive strength of samples consumes time, finance, and labor. Computerized methods could help decrease the compressive strength estimation cost for different mixture designs of concretes [24,25]. Dao et al. developed ANN and ANFIS based prediction models to estimate the prediction of compressive strength. They employed 210 samples to put forward the precise estimation of geopolymer concrete compressive strength [27]. In another study, Ilker and Mustafa provided a prediction model to determine compressive strength. For this aim, they used 52 different concrete mixtures with fly ash, which ended in 180 samples[28]. Ali et al., in their study, computed the mechanical features of concrete containing compressive strength, tensile strength, and flexural strength for roller compacted concrete pavement. They applied classification-based regression models such as random forest and M5 prime models to implement the prediction of mentioned properties [29]. Saridemir also used a multi-layer neural network to predict concrete's compressive strength, including micro-silica. He employed 195 samples with 33 various mixture designs. This feedforward multi-layer network provided a robust prediction of compressive strength[30]. Pazuki et al. the compressive strength was determined using an RBFNN neural network. They supplied 327 SCC samples, including CFFA, to generate predictive models. [31].

**Table 1.** descriptive analysis results of parameter features

| Phase | Variables | Abbr | Description of Variables | | | |
|---|---|---|---|---|---|---|
| | | | Min | Max | Ave | St. dev |
| Input | Binder (kg) | B | 394 | 500 | 418.381 | 40.017 |
| | Fly ash to Binder ratio | FA/B | 0 | 0.55 | 0.2411 | 0.1482 |
| | Micro-silica to binder ratio | MS/B | 0 | 0.1099 | 0.0543 | 0.0452 |
| | Superplasticizer to binder ratio (%) | SP/B | 0 | 2.6 | 1.034 | 0.6226 |
| | Coarse aggregates to binder ratio | CA/B | 2.172 | 2.906 | 2.736 | 0.2789 |
| | Coarse aggregate to total aggregate ratio | CA/TA | 0.6 | 0.6787 | 0.6283 | 0.0204 |
| | Water to binder ratio | W/B | 0.3 | 0.5 | 0.4 | 0.0816 |
| | Curing time (days) | CT | 28 | 180 | 68.571 | 49.836 |
| Target | Compressive strength (MPa) | CS | 24 | 107.8 | 64.032 | 15.309 |

The CS is one of the concrete's main features, which has a significant effect on the strength of concrete membranes. The researcher develops many artificial-based methods to facilitate the prediction of compressive in terms of time and financial cost. On the other hand, various supplementary are applied to enhance the compressive strength. Fly ash and micro-silica are supplementary materials that increase compressive strength and durability. Employing different parentage of these by-product materials in substitution of cement in concrete helps produce high-performance concrete (HPC).

The present study develops a precise prediction model based on a radial base function neural network (RBFN). In the process of predicting the compressive strength, a different mixture of concrete containing fly ash and micro-silica combined with various percent of superplasticizer were considered to figure out the effects of mentioned admixtures in the compressive strength of HPC concrete.

The method's accuracy is enhanced by using two metaheuristic optimization algorithms (arithmetic optimization algorithm and antlion optimization algorithm) coupled with RBFN, AORBFN, and ALRBFN. A dataset containing B (binder) (kg/m3), FA (fly ash) (kg/m3), MS (micro-silica) (kg/m3), CA (coarse aggregate) (kg/m3), TA (total aggregate) (kg/m3), W (water) (kg/m3), SP (superplasticizer) (kg/m3), CT (curing time) (days), and CS (compressive strength) (Mpa) With different mixtures design are applied to implement hybrid proposed models. Moreover, statistical evaluators such as $R^2$, RMSE, NMSE, VAF, and MDAPE are utilized to maintain the robustness of two hybrid models and compare models.

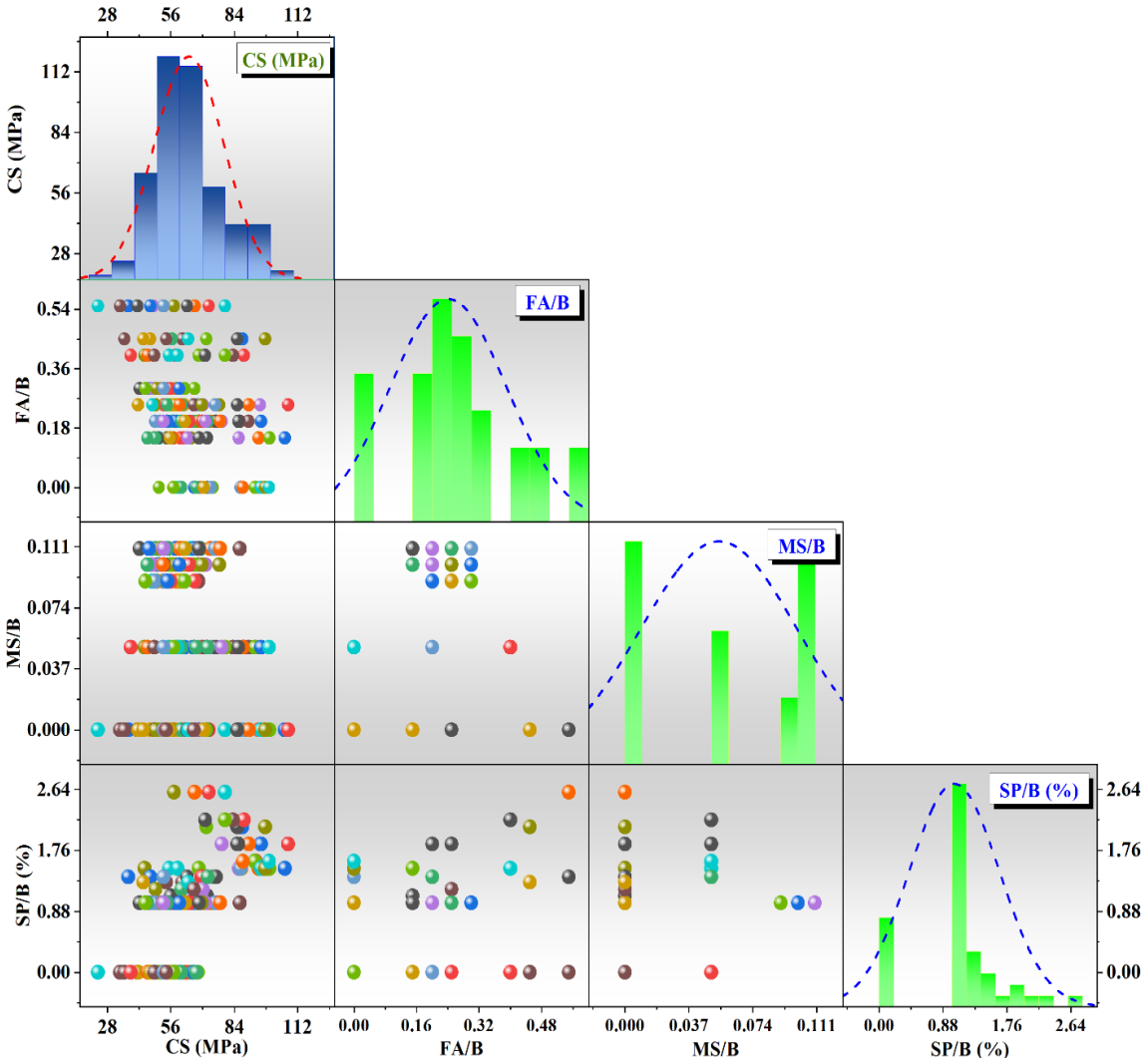


**Fig. 1**. The scatter matrix plot and distribution plot of impressive input and output compressive strength

## 2. Methodology

### *2.1.Materials*

A collection of data three sets of concrete mix designs divided by water to binder ratio of 0.3,0.4, and 0.5. The binder material is ASTM Type 1 Portland cement, fly ash is a low calcium type conforming to ASTM Class F, and micro-silica is commercially available. The present collection of the dataset is driven from the literature [32]. Binder, micro-silica to binder ratio, fly ash to binder ratio, coarse aggregate to total aggregate ratio, coarse aggregate to binder ratio, high-rate water reducing agent to binder ratio, water to binder ratio, curing time (days) and compression strength. Various mixed designs of HPC concrete including micro-silica and fly ash are used, taking into account the proportion of high-rate water reducing agents. Fig.1 displays the scatter plot of fly ash, micro-silica, and superplasticizer in proportion to compressive strength. Moreover, the distribution of the three abovementioned admixtures is depicted in Fig.1. Also, an illustration of input variables attributes is listed in Table.1. Fig.1 provides the

histogram of input and target variable of model and their distribution according to normal distribution. Also, the correlation between the inputs and target is depicted as color nodes.

### *2.2. Radial basis function (RBF)*

Radial basis function (RBF) neural networks are classified as feedforward models trained by supervised learning algorithms [33]. This neural network containing three main layers: an input, a hidden, and an output. In the input layer, the neurons' number is set equal to the number of inputs, and those nodes do not calculate [34]. The hidden layer node function is the Radial Basis Function (RBF), which performs non-linear the input layer's mapping. The main action of the RBF is to compute the apace of an input variable with a midpoint that depends on the symmetry property.

In the output layer, a non-linear projection of the hidden layer's input parameters integrates the hidden layer's output into the output layer by linear regression. Number of radial basis functions are used like sigmoid, Gaussian, barely poly-secondary and inverse poly-secondary. The most commonly used radial basis function is a Gaussian function with central diffusivity and features.[35].

The first RBFN process calculated the distance between the input vector and the center point of each node in the hidden layer. The next step is to use the RBF function to determine the output of each node.

$$D_i = \|X - C_i\| \tag{1}$$

$$O_i = Gau(D_i . \sigma_i \tag{2}$$

Where $D_i$ is the radial distance between input vector $(X)$ and center point $(C_i)$ of node $i$ in the hidden layer. $O_i$ is the output of $i-th$ RBF node determined by Gaussian RBF function $(Gau)$. In addition, $\sigma_i$ shows the $i-th$ node's width.

The output layer can be described in the following:

$$CS = f(X) = \sum_{i=1}^{m} W_i O_i \tag{3}$$

Therefore, $m$ defines the largest neuron in the hidden layer and $W_i$ describes the weight between the node in the output layer and the node $i$ in the hidden layer. The structure of the RBF is shown in Figure

Determining the rate of propagation and the hidden layer's number neurons in the structure of the RBF model is very important. In this study, determine both parameters through the presenting new metaheuristic method.

### *2.3. Arithmetic optimization algorithm (AOA)*

AOA is a candidate-based algorithm with the conception of algebra that uses arithmetic operators to find and update new positions in the population without calculating results [35].Arithmetic is a major part of modern mathematics and one of the foundations of number theory. The algorithm process begins with the initialization of randomly generated solution candidates.

$$C = \begin{bmatrix} c_{1,1} & \cdots & c_{1,j} \\ \vdots & \ddots & \vdots \\ c_{N,1} & \cdots & c_{N,j} \end{bmatrix} \tag{4}$$

The algorithm includes two main sections: search and utilization. After developing the first candidate, need to define an exploration space for the search or utilization and implement it utilizing the Mathematical Optimizer Accelerator Function (MOA).

$$MOA = Min + iter \times (\frac{Max - Min}{Max_{iter}}) \tag{5}$$

Here, the minimum and maximum values for the MOA describe with $Min$ and $Max$ . $iter$ indicates the current repetition and $Max_{iter}$ shows the maximum number of iterations.

The search operation performs on highly spread values and applies arithmetic multiplication (M) and division (D) operators to the search operation. M and D are highly volatile and do not help achieve the goal, though using the arithmetic operator subtraction (S). If $r_1 > MOA$ the search step of the algorithm is in progress. The location of the search phase is updated employing Eq. 6 which utilizes the M and D operators.

$$c(iter+1)_{i,j} = \begin{cases} best(c_j) \div (MOP + \varepsilon) \times \left((ub - lb) \times \mu + lb\right) \\ r_2 > 0.5 \\ best(c_j) \div (MOP) \times \left((ub - lb) \times \mu + lb\right) \\ otherwise \end{cases} \tag{6}$$

Here, $best(c_j)$ shows the global best location, $lb\ and\ ub$ are the lower and upper bound of the exploration space. $\varepsilon$ indicates little value, and $\mu$ sets the control parameters for the exploration method, which is set to 0.499 in this study. MOP represented as a mathematical optimization possibility and computed in the following:

$$MOP(iter) = 1 - \frac{iter^{1/\alpha}}{Max_{iter}{}^{1/\alpha}} \tag{7}$$

In the above equation, parameter $\alpha$ shows the sensitivity parameter for accuracy during iteration and is equal to 5.

Moreover, if $r_1 < MOA$ the abuse phase occurs. In this step, the arithmetic operators S and A are used to the deep

dense domain search. This depth-first exploration is modeled in the following:

$$c(iter+1)_{i,j} = \begin{cases} best(c_j) - (MOP) \times ((ub - lb) \times \mu + lb) & r_3 > 0.5 \\ best(c_j) + (MOP) \times ((ub - lb) \times \mu + lb) & otherwise \end{cases} \quad (8)$$

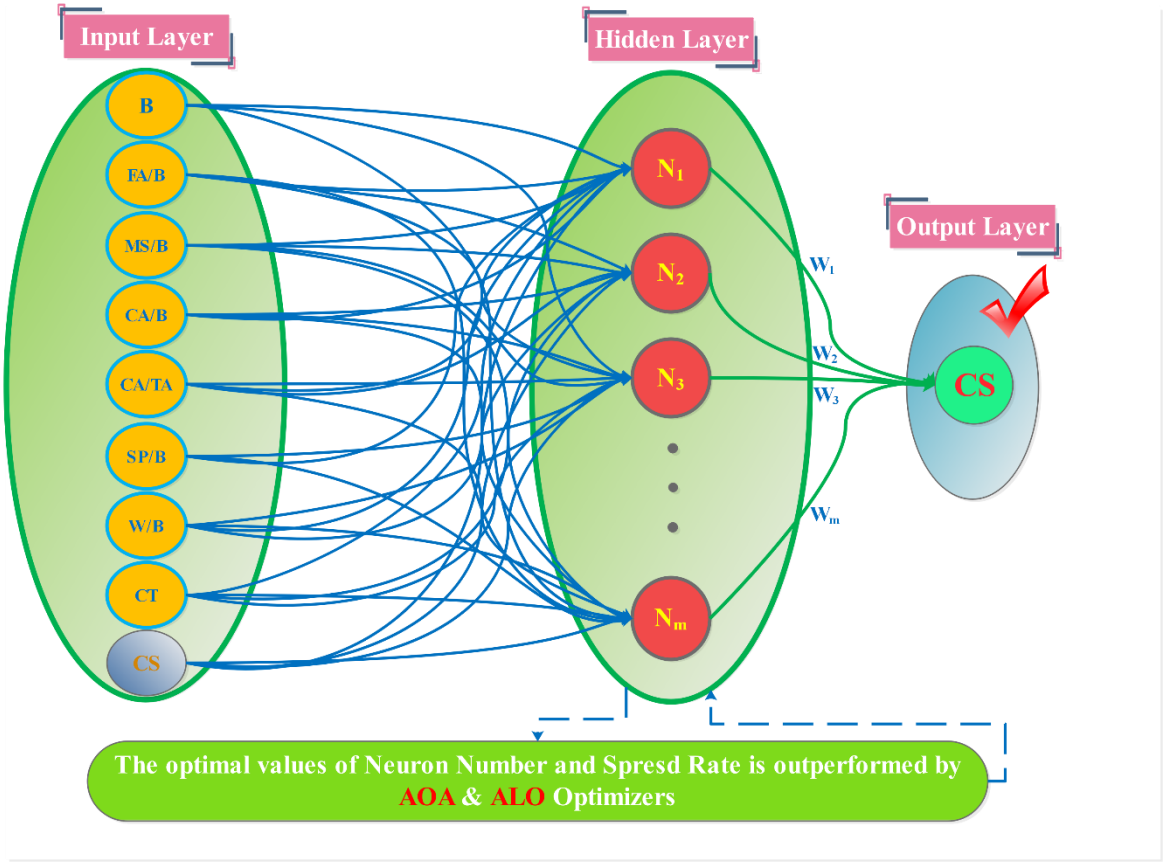


**Fig. 2.** schematic flowchart of hybrid radial base neural network

### *2.4. Antlion optimization algorithm (ALO)*

The antlion optimization algorithm is also a population-based optimization algorithm built on the demeanor of the antlion in its life cycle [35]. The stop criterion for this algorithm is the repetition's number, which finds the best result for the entire iteration. This algorithm's main part is to develop first candidates for antlion and ants. The method by which antlion hunts ants and updates the positions of ants and antlion can be summarized in the following:

- Prey's random walk
- Create a trap
- Catch the prey and press it against the antlion (AL)
- Elite AL selection

Cumulative totals are employed to describe the location of bred ants in the following:

$$X(t) = [0, C_{sum}(2r(t_1)) - 1, \dots, C_{sum}(2r(t_n)) - 1] \quad (9)$$

$$r(t) = \begin{Bmatrix} 1, rand(0,1) > 0.5 \\ 0, rand(0,1) \le 0.5 \end{Bmatrix} \quad (10)$$

The normalization process is utilized in each repetition.

$$X_i^t = \frac{(X_i^t - a_i).(d_i^t - c_i^t)}{b_i - a_i} + c_i^t \quad (11)$$

$d_i^t$ the presented variable's maximum

$c_i^t$ the presented variable minimum

$b_i$ random walk in the i^th variable' maximum

$a_i$ random walk in the i^th variable' minimum

The Prey's Random Walk is involved by the AL holes shown as follows.

$$X(t) = [0, C_{sum}(2r(t_1)) - 1, \dots, C_{sum}(2r(t_n)) - 1] \quad (12)$$

$$X(t) = [0, C_{sum}(2r(t_1)) - 1, \dots, C_{sum}(2r(t_n)) - 1] \quad (13)$$

$Antlion_j^t$ the $j^{th}$ AL's position

$d^t$ vectors including the variable maximum

$c^t$ vectors including the variables minimum

Prey execution donates to AL's performance because AL is supposed to catch prey. Thus, can apply Roulette Wheel Selection (RWS). Based on this concept, the prey with the highest fitness value is most likely to catch a good prey. By equations 14 and 15, the preys' behavior slipping into a trap is mathematically modeled.

$$c^t = \frac{c^t}{I} \quad (14)$$

$$d^t = \frac{d^t}{I} \quad (15)$$

The parameter *I* of the equation for the ratio depended on the maximum and current repetition. Trap searches reduce the area and help converge on the optimal solution. According to the prey and AL's fitness values, the next step is to select the elite antlion.

$$f(Ant_i^t) < f(Antlion_j^t) \rightarrow Antlion_j^t = Ant_i^t \quad (16)$$

$R_A^t$ determined the prey's random walk around the antlion and $R_E^t$ is indicates a prey's random walk around the elite antlion. The location of the ant considering the values of $R_A^t$ and $R_E^t$ is defined below:

$$Ant_i^t = \frac{R_A^t + R_E^t}{2} \quad (17)$$

### *2.5. Statistical indicators*

Statistical evaluators are expected to find the robustness of the both new hybrid models (AORBFN and ALRBFN) and provide a comprehensive comparison of models.

- Coefficient of determination ($R^2$):

$$R^2 = \left( \frac{\sum_{n=1}^{N}(t_n - \bar{t})(p_n - \bar{p})}{\sqrt{[\sum_{n=1}^{N}(t_n - \bar{p})^2][\sum_{n=1}^{N}(p_n - \bar{p})^2]}} \right)^2 \quad (18)$$

- Root mean squared error (RMSE):

$$RMSE = \sqrt{\frac{1}{N}\sum_{n=1}^{N}(t_n - p_n)^2} \quad (19)$$

- Normalized mean squared error (NMSE):

$$NMSE = \frac{1}{N}\sum_{n=1}^{N}\frac{(t_n - p_n)^2}{t_n * p_n} \quad (20)$$

- Median of absolute percentage error:

$$MDAPE = median\left(\left\|\frac{t_n - p_n}{t_n}\right\| \times 100\%\right) \quad (21)$$

- Variance account factor

$$VAF = \left(1 - \frac{var(t_n - p_n)}{var(t_n)}\right) * 100 \quad (22)$$

Here $p_n$ and $t_n$ are predicted and measured values, respectively. $N$ shows the samples' total number. $\bar{p}$ and $\bar{t}$, describe the mean value of predicted and measured parameters, respectively.

**Table 2.** Results evaluation of two hybrid proposed models based on statistical metrics.

| **Statistical Metrics** | **Prediction models** | | | |
|---|---|---|---|---|
| | **AORBF** | | **ALRBF** | |
| | **Train** | **Test** | **Train** | **Test** |
| **$R^2$** | 0.9686 | 0.9706 | 0.9559 | 0.9669 |
| Rank | 3 | 4 | 1 | 2 |
| **RMSE (Mpa)** | 2.5886 | 2.9010 | 3.0714 | 3.1044 |
| Rank | 4 | 3 | 2 | 1 |
| **NMSE** | 6.6437 | 8.2991 | 9.4805 | 9.2445 |

| | | | | |
|---|---|---|---|---|
| Rank | 4 | 3 | 1 | 2 |
| **MDAPE (Mpa)** | 2.8726 | 2.9294 | 3.7124 | 3.8439 |
| Rank | 4 | 3 | 2 | 1 |
| VAF | 96.7121 | 97.0153 | 95.3829 | 96.5500 |
| Rank | 3 | 4 | 1 | 2 |
| Total rank | 18 | 17 | 7 | 8 |

## 3. Results and discussions

The high-volume consumption of concrete in construction industries, the cost of materials, and the environmental effects of producing concrete provoke researchers and manufacturers to pay attention to a novel mixture of high-performance concrete. The important constraints in new are to minimize the usage of materials such as cement, diminish the emission of carbon dioxide, and decrease the financial cost of concrete. A well-known way to produce HPC concrete is by applying by-product admixtures to the mix design of HPC concrete. Fly ash and micro-silica recently are in the attention zone of researchers and industrial concrete manufacturers. The critical issue in using these supplementary materials is to figure out their impacts on the concrete mechanical properties, especially the CS.

In this study, a precise collection of various mix designs is employed to evaluate the effects of fly ash and micro-silica on CS. Different mix designs of fly ash and micro-silica coupled with superplasticizer are considered for this aim. As mentioned, considering the financial, environmental, laboring, and time cost of determining the compressive strength by the experimental method, forces to implement the estimation of compressive strength by the artificial neural network. Two tuned models based on RBFN were developed to accomplish the prediction process in the present study. The RBFN models are tuned by arithmetic and antlion optimization algorithms to build AORBFN and ALRBFN, respectively. The provided dataset contains binder (B (kg)) binder, micro-silica/binder ratio (MS/B), fly ash/binder ratio (FA/B), coarse aggregate/total aggregate ratio (CA/TA), coarse aggregate/binder ratio (CA/B), superplasticizer/binder (SP/B (%)), water/binder (W/B), and curing time (CT (days)) as input parameters and compressive strength (CS) as target values employed. Also, the dataset was divided to the training and testing phases by the proportion of 70% and 30%. The dataset is randpermed using normal distribution function then the mentioned ratios of input generate to eliminate the dimension of input data. First 70 % of data was applied to debug the training phase, then the best trained network was validated in the testing phase by the rest 30% of the data. Several statistical evaluators such as $R^2$, RMSE, NMSE, MDAPE, and VAF preferred to figure out the best developed hybrid model in the training phase and evaluate the selected model's validation in the testing phase.

The robustness of the model is also validated considering precise work in literature performed by Yin et al. [38], which utilized the same data set to promote their prediction model of compressive strength. Evaluating the RMSE index, the RMSE's best value for the model developed by Yin et al. is 4.8756, whereas the RMSE's worst value for present work is about 3.1044. as it is clear, the present work provides a robust model with acceptable output results.

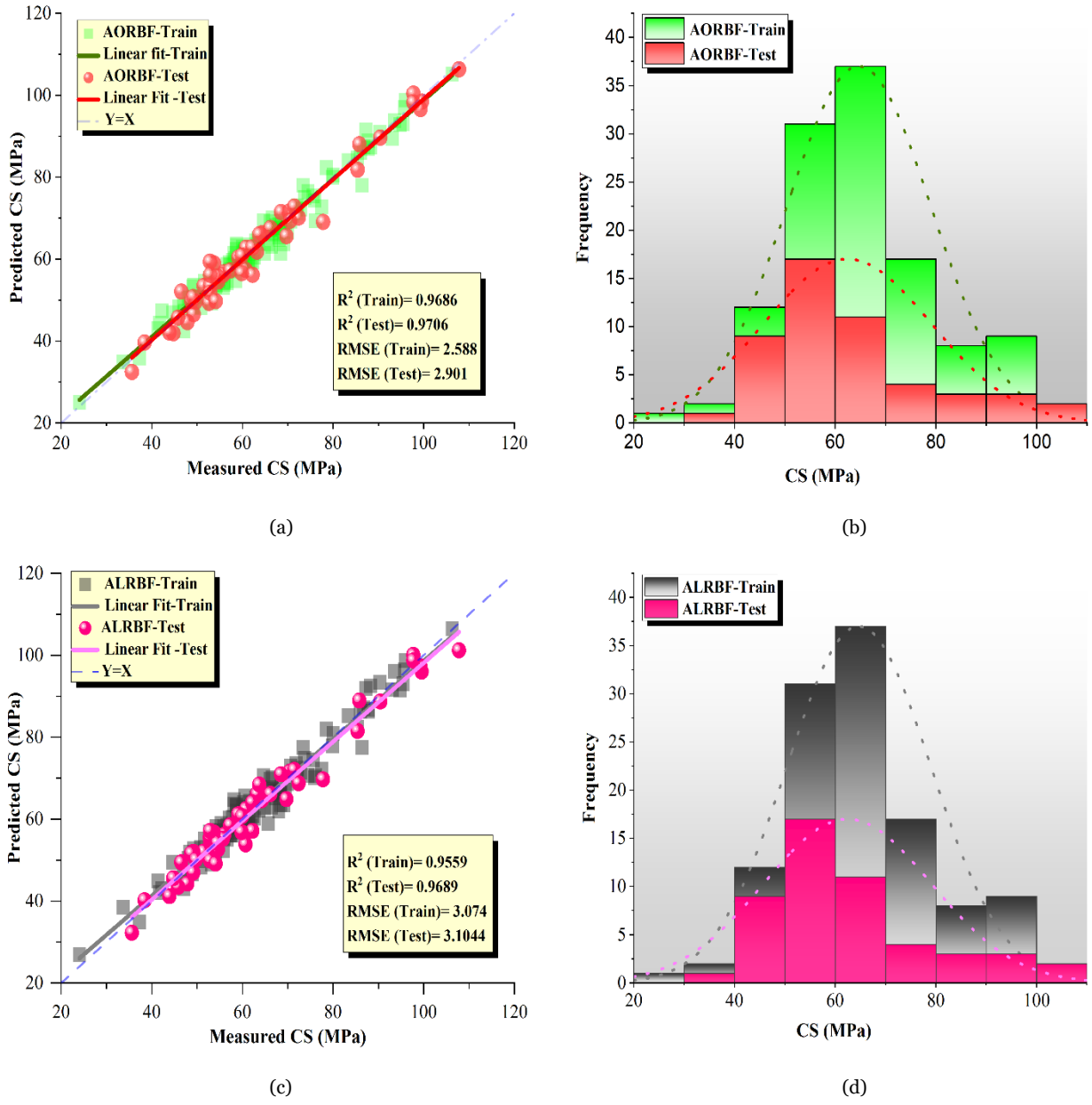


**Fig 3**. The correlation plot and distribution plot of hybrid proposed models: a) AORBF scatter plot b) AORBF histogram c) ALRBF scatter plot d) ALRBF histogram

As cleared above, the AORBFN model and the ALRBFN model were utilized for the training and test phase, and the output of these novel hybrid models was evaluated through the abovementioned statistical indices. Table.2 present the output results of the two models in detail. As shown in Table.2, the best RMSE value is taken by the AORBF model in the training phase, and the second stage of RMESE is for the same model in the testing step. The ALRBFN model also performed an acceptable prediction of compressive strength considering RMSE. Another index to evaluate the performance of the models is $R^{2,}$ where the values of this index for the training and test phase of both the AORBFN and ALRBFN model are reported as 0.9689, 0.9706, 0.9559, and 0.9669, respectively. The best value for this index is for AORBFN in the test phase, and the worst is for ALRBFN in the training phase. MDAPE is also showed the same trend as RMASE, with the best value of 2.8726 for AORBFN in the training phase and the worst value of 3.8439 for the ALRBFN model in the test phase. The NMSE index shows different feedback of the model. the first stage considering NMSE is for AORBF in the training phase with the value of 6.6437 and the last stage is for ALRBFN in the same phase with the value of 9.4805. moreover, the VAF index showed a

reaction trend same as $R^2$ with the values of 96.7121, 97.0153, 95.3829, and 96.55 for the training and test section of AORBFN and ALRBFN, respectively.

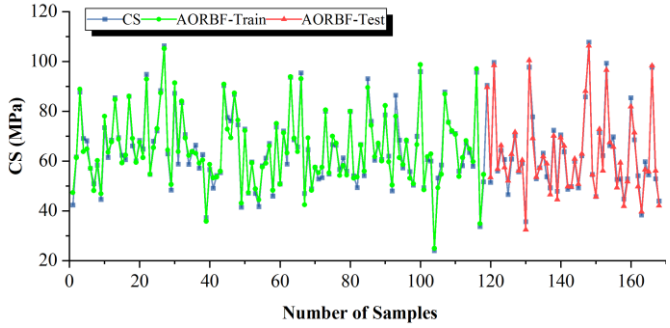


(a)

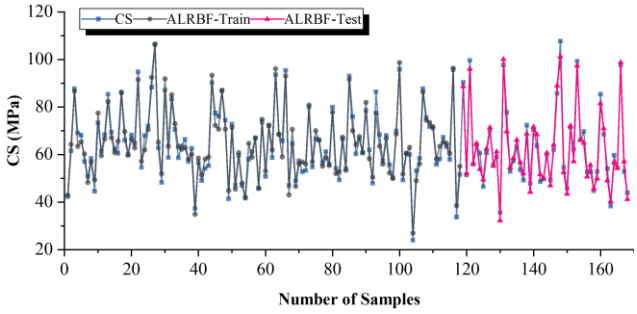


(b)

**Fig 4.** the time series distribution of AORBF and ALRBF models: a) AORBF b) ALRBF

The employed ranking system also demonstrates that the AORBFN model in the training phase outperforms the best predicting model. The second, third, and fourth stages belong to AORBFN in the test phase, ALRBFN in the test phase, and ALRBFN in the training phase.

Fig.3 provides the distribution of the hybrid models for the training and test phase. Also, the correlation plots of proposed models are depicted in Fig.3. as Figs.3(a-d) shows, both models in both phases provide an acceptable correlation between the predicted and measured values of compressive strength. Considering the fitted line for the training and test data, it is evident that the best correlation is obtainable from the AORBFN model. Meanwhile, the distribution diagrams indicate the partially identical performance of the models.

A comprehensive understanding of the model potential in predicting compressive strength values is achievable from time series plots drawn for AORBFN and ALRBFN models in Fig.4. as Figs.4(a-b) AORBF model supplies an acceptable behavior for predicting compressive strength in both sections. It is evident that comparing the AORBF and ALRBF models, the AORBF model predicted values best matches the measured values, and the lowest deviation of compressive strength values is obtained for the AORNFN model.

## 4. Conclusion

In the present study, the effect of fly ash and micro-silica on the compressive strength of HPC concrete was investigated. For this aim, two hybrid models based on RBFN were developed and tuned by ALO and AOA optimization algorithms to reach the optimal accuracy of the provided network in predicting compressive strength values. It is demonstrated that prediction of compressive strength based on artificial intelligence method delivers a beneficial model in terms of environmental, financial, and time cost. The following outsets of this work can be drawn as:

- Two novel hybrid models named AORBFN and ALRBFN were developed. The AORBFN model outperformed best between developed models.
- In both models, the optimum values of the spread rate and the maximum number of RBF neurons in the hidden layer are set by the coupled optimization algorithm.
- The training phase of the AORBFN model performed best in predicting compressive strength.
- Both models demonstrated their precise capability of predicting the compressive strength of HPC concrete, and the AORBF model can be introduced as the most workable model.

## REFERENCES


[1] Eskandari-Naddaf H, Kazemi R. ANN prediction of cement mortar compressive strength, influence of cement strength class. Construction and Building Materials 2017; 138:1–11.

[2] Li LG, Huang ZH, Zhu J, Kwan AKH, Chen HY. Synergistic effects of micro-silica and nano-silica on strength and microstructure of mortar. Construction and Building Materials 2017; 140:229–38.

[3] Cho YK, Jung SH, Choi YC. Effects of chemical composition of fly ash on compressive strength of fly ash cement mortar. Construction and Building Materials 2019; 204:255–64. https://doi.org/10.1016/j.conbuildmat.2019.01.208.

[4] Lezgy-Nazargah M, Emamian SA, Aghasizadeh E, Khani M. Predicting the mechanical properties of ordinary concrete and nano-silica concrete using micromechanical methods. Sādhanā 2018; 43:196. https://doi.org/10.1007/s12046-018-0965-0.

[5] Hansen TC. Long-term strength of high fly ash concretes. Cement and Concrete Research 1990;

20:193–6. https://doi.org/10.1016/0008-8846(90)90071-5.
[6] Lu P, Chen S, Zheng Y. Artificial Intelligence in Civil Engineering. Mathematical Problems in Engineering 2012; 2012:1–22. https://doi.org/10.1155/2012/145974.
[7] Ganesh BK, Siva NRG. Efficiency of fly ash in concrete with age. Cement and Concrete Research 1996; 26:465–74.
[8] Ganesh Babu K, Siva Nageswara Rao G. Early strength behaviour of fly ash concretes. Cement and Concrete Research 1994; 24:277–84. https://doi.org/10.1016/0008-8846(94)90053-1.
[9] Lam L, Wong YL, Poon CS. Effect of Fly Ash and Silica Fume on Compressive and Fracture Behaviors of Concrete. Cement and Concrete Research 1998; 28:271–83. https://doi.org/10.1016/S0008-8846(97)00269-X.
[10] Sabir BB. Mechanical properties and frost resistance of silica fume concrete. Cement and Concrete Composites 1997; 19:285–94. https://doi.org/10.1016/S0958-9465(97)00020-6.
[11] Mazloom M, Ramezanianpour AA, Brooks JJ. Effect of silica fume on mechanical properties of high-strength concrete. Cement and Concrete Composites 2004; 26:347–57. https://doi.org/10.1016/S0958-9465(03)00017-9.
[12] Bajja Z, Dridi W, Darquennes A, Bennacer R, Le Bescop P, Rahim M. Influence of slurried silica fume on microstructure and tritiated water diffusivity of cement pastes. Construction and Building Materials 2017; 132:85–93. https://doi.org/10.1016/j.conbuildmat.2016.11.097.
[13] Rostami M, Behfarnia K. The effect of silica fume on durability of alkali activated slag concrete. Construction and Building Materials 2017; 134:262–8. https://doi.org/10.1016/j.conbuildmat.2016.12.072.
[14] Li H, Xiao H, Yuan J, Ou J. Microstructure of cement mortar with nano-particles. Composites Part B: Engineering 2004; 35:185–9. https://doi.org/10.1016/S1359-8368(03)00052-0.
[15] Singh LP, Karade SR, Bhattacharyya SK, Yousuf MM, Ahalawat S. Beneficial role of nanosilica in cement-based materials – A review. Construction and Building Materials 2013; 47:1069–77. https://doi.org/10.1016/j.conbuildmat.2013.05.052.
[16] Mukhopadhyay AK. Next-Generation Nano-based Concrete Construction Products: A Review. Nanotechnology in Civil Infrastructure, Berlin, Heidelberg: Springer Berlin Heidelberg; 2011, p. 207–23. https://doi.org/10.1007/978-3-642-16657-0_7.
[17] Li LG, Zheng JY, Zhu J, Kwan AKH. Combined usage of micro-silica and nano-silica in concrete: SP demand, cementing efficiencies and synergistic effect. Construction and Building Materials 2018; 168:622–32. https://doi.org/10.1016/j.conbuildmat.2018.02.181.
[18] Norhasri MSM, Hamidah MS, Fadzil AM. Applications of using nano material in concrete: A review. Construction and Building Materials 2017; 133:91–7. https://doi.org/10.1016/j.conbuildmat.2016.12.005.
[19] Rashad AM. A comprehensive overview about the effect of nano-SiO2 on some properties of traditional cementitious materials and alkali-activated fly ash. Construction and Building Materials 2014; 52:437–64. https://doi.org/10.1016/j.conbuildmat.2013.10.101.
[20] Shaikh FUA, Shafaei Y, Sarker PK. Effect of nano and micro-silica on bond behaviour of steel and polypropylene fibres in high volume fly ash mortar. Construction and Building Materials 2016; 115:690–8. https://doi.org/10.1016/j.conbuildmat.2016.04.090.
[21] Jalal M, Pouladkhan A, Harandi OF, Jafari D. Comparative study on effects of Class F fly ash, nano silica and silica fume on properties of high performance self-compacting concrete. Construction and Building Materials 2015; 94:104.
[22] Li LG, Zhu J, Huang ZH, Kwan AKH, Li LJ. Combined effects of micro-silica and nano-silica on durability of mortar. Construction and Building Materials 2017; 157:337–47. https://doi.org/10.1016/j.conbuildmat.2017.09.105.
[23] Sarıdemir M. Effect of specimen size and shape on compressive strength of concrete containing fly ash: Application of genetic programming for design. Materials & Design (1980-2015) 2014; 56:297–304. https://doi.org/10.1016/j.matdes.2013.10.073.
[24] Eskandari-Naddaf H, Kazemi R. ANN prediction of cement mortar compressive strength, influence of cement strength class. Construction and Building Materials 2017; 138:1–11. https://doi.org/10.1016/j.conbuildmat.2017.01.132.
[25] Özcan F. Gene expression programming-based formulations for splitting tensile strength of concrete. Construction and Building Materials 2012; 26:404–10. https://doi.org/10.1016/j.conbuildmat.2011.06.039.
[26] Topçu İB, Sarıdemir M. Prediction of compressive strength of concrete containing fly ash using artificial neural networks and fuzzy logic. Computational Materials Science 2008; 41:305–11. https://doi.org/10.1016/j.commatsci.2007.04.009.
[27] Dao D, Trinh S, Ly H-B, Pham B. Prediction of Compressive Strength of Geopolymer Concrete

Using Entirely Steel Slag Aggregates: Novel Hybrid Artificial Intelligence Approaches. Applied Sciences 2019; 9:1113. https://doi.org/10.3390/app9061113.
[28] Ashrafian A, Taheri Amiri MJ, Masoumi P, Asadi-shiadeh M, Yaghoubi-chenari M, Mosavi A, et al. Classification-Based Regression Models for Prediction of the Mechanical Properties of Roller-Compacted Concrete Pavement. Applied Sciences 2020; 10:3707. https://doi.org/10.3390/app10113707.
[29] Pazouki G, Golafshani EM, Behnood A. Predicting the compressive strength of self-compacting concrete containing Class F fly ash using metaheuristic radial basis function neural network. Structural Concrete 2021. https://doi.org/10.1002/suco.202000047.
[30] Lam L, Wong YL, Poon CS. Effect of Fly Ash and Silica Fume on Compressive and Fracture Behaviors of Concrete. Cement and Concrete Research 1998; 28:271–83. https://doi.org/10.1016/S0008-8846(97)00269-X.
[31] Broomhead DS, Lowe D. Radial basis functions, multi-variable functional interpolation and adaptive networks. Royal Signals and Radar Establishment Malvern (United Kingdom); 1988.
[32] Sonebi M. Medium strength self-compacting concrete containing fly ash: Modelling using factorial experimental plans. Cement and Concrete Research 2004; 34:1199–208. https://doi.org/10.1016/j.cemconres.2003.12.022.
[33] Luan F, Zhang XY, Zhang HX, Zhang RS, Liu MC, Hu ZD, et al. QSPR study of permeability coefficients through low-density polyethylene based on radial basis function neural networks and the heuristic method. Computational Materials Science 2006; 37:454–61. https://doi.org/10.1016/j.commatsci.2005.11.003.
[34] Armaghani DJ, Asteris PG, Fatemi SA, Hasanipanah M, Tarinejad R, Rashid ASA, et al. On the Use of Neuro-Swarm System to Forecast the Pile Settlement. Applied Sciences 2020; 10:1904. https://doi.org/10.3390/app10061904.
[35] Yin H, Liu S, Lu S, Nie W, Jia B. Prediction of the compressive and tensile strength of HPC concrete with fly ash and micro-silica using hybrid algorithms. Advances in Concrete Construction 2021; 12:339–54.